Geogr. Fis. Dinam. Quat.
41 (2018). 67-81, 9 figg, 1 tab.

DOI 10.4461/ GFDQ.2018.41.5

SALVATORE IVO GIANO [1*], LUCIANA MECCA [1], STEFANIA PASCALE [1]
& MARCELLO SCHIATTARELLA [2]

MORPHOMETRIC ANALYSIS OF THE THRUST FRONT OF THE LUCANIAN APENNINE, SOUTHERN ITALY

ABSTRACT: GIANO S.I., MECCA L., PASCALE S. & SCHIATTARELLA M., *Morphometric analysis of the thrust front of the Lucanian Apennine, southern Italy.* (IT ISSN 0391-9838, 2018).

The thrust front of the southern Italian Apennines is formed by a north-east verging imbricate fan, transversally cut by several major rivers draining to the Ionian Sea. In the Lucanian segment of this frontal (i.e. external) part of the orogen, the tectonic stack is composed of Cretaceous-Oligocene deep-sea water clayey successions and Miocene siliciclastic units that was embedded during Neogene and Quaternary times. Currently, it is still debated if the recent contractional deformation continued until now in this external part of the orogenic chain. In fact, field data show a recent shortening not younger than the Middle Pleistocene. On the other hand, geomorphological features clearly indicate that the whole area suffered a significant uplift in more recent times. This study will try to discriminate the recent and active tectonic deformation in the light of an accurate morphotectonic analysis, based both on the study of terraced surfaces and morphometric indices. The analysis of fluvial terraces revealed that the study area underwent a diffused uplift during the Late Pleistocene. In the Holocene, the same area seems to be affected by a differential uplift due to tectonic tilting toward south-east, as also supported by the increase of the sinuosity index (SI) of the Bradano River. The tectonic imprint on the landscape has been adequately proved by other indices such as the asymmetry index (AF), the valley floor slope (VF_s), and the normalized stream length-gradient index (SL_k). The mapping of SL_k values has also shown that the anomalies follow a NW-SE trend, suggesting a very recent activity of the external ridges. Moreover, swath profile analysis has shown altimetrical peaks that are topographically corresponding to the main outcropping thrust and more external buried structures located in the foredeep. The geomorphic analysis led to the consideration that the frontal portion of the Lucanian Apennine is still tectonically active, even though its recent evolution has not been laterally uniform.

[1] *Dipartimento di Scienze, Basilicata University, I-85100 Potenza, Italy.*
[2] *Dipartimento delle Culture Europee e del Mediterraneo (DiCEM), Basilicata University, I-75100 Matera, Italy.*

* *Corresponding author: S.I. GIANO, ivo.giano@unibas.it*

This study was financially supported by Basilicata University RIL 2015 granted to S.I. Giano and M. Schiattarella. Many thanks to the anonymous referees for helpful comments and to Marcella D'Amico, appointed lecturer at the Basilicata University, for the English revision of the final text.

KEY WORDS: Tectonic geomorphology, Geomorphometry, Active thrusting, Lucanian Apennine, Bradano Foredeep, Southern Italy.

RIASSUNTO: GIANO S.I., MECCA L., PASCALE S. & SCHIATTARELLA M., *Analisi morfometrica del fronte di sovrascorrimento dell'Appennino lucano (Italia meridionale).* (IT ISSN 0391-9838, 2018).

La fascia esterna dell'Appennino meridionale, limitata ad est dal fronte della catena e dall'adiacente avanfossa, è formata da un ventaglio embricato di sovrascorrimenti attraversato in discordanza da diversi corsi d'acqua maggiori che drenano verso il Mar Ionio. Nel segmento lucano della porzione frontale dell'orogene, le unità tettoniche sono costituite da successioni a dominante argillosa cretacico-oligoceniche e dai "flysch esterni" miocenici, impilate durante il Neogene e il Quaternario. È però ancora oggetto di discussione se la tettonica compressiva sia ancora attiva in questo settore della catena, poiché mancano chiare evidenze di raccorciamento di età successiva al Pleistocene medio. D'altro canto, i caratteri geomorfologici dell'area indicano chiaramente un significativo sollevamento in tempi più recenti. Questo studio si propone di discriminare le diverse componenti della deformazione recente e attiva in un'area sufficientemente ampia del fronte della catena, attraverso gli strumenti dell'analisi morfotettonica e morfometrica.

L'analisi della distribuzione spaziale dei terrazzi fluviali e dei loro profili longitudinali in comparazione con quello dell'alveo attuale del Fiume Bradano ha rivelato che l'area è stata interessata da un sollevamento generalizzato durante il Pleistocene superiore. Nell'Olocene, l'area di studio sembra invece aver subito un *uplift* differenziale generato da un complessivo basculamento tettonico verso sud-est, come denunciato dall'incremento del valore dell'indice di sinuosità (SI) del Fiume Bradano. Un simile comportamento è ampiamente dimostrato da altri parametri geomorfici quali l'indice di asimmetria valliva (AF), il gradiente di pendio del fondovalle (VF_s) e l'indice SL_k (*normalized stream length-gradient index*). La carta derivata dal calcolo dei valori di SL_k ha inoltre mostrato che le anomalie nella distribuzione dell'indice seguono un andamento NO-SE, suggerendo un'attività tettonica molto recente dell'area frontale della catena. Un risultato comparabile è fornito dall'interpretazione degli *swath profile*, che evidenzia l'esistenza di difformità tra le curve topografiche in corrispondenza del sovrascorrimento sepolto principale e di *thrust* ciechi più esterni, collocati in avanfossa. Pertanto, l'analisi geomorfologica dell'area del fronte della catena sudappenninica permette di considerare quella porzione della catena come tettonicamente attiva, anche se la sua evoluzione non è stata lateralmente uniforme.

TERMINI CHIAVE: Geomorfologia tettonica, Geomorfometria, Sovrascorrimenti attivi, Appennino meridionale, Avanfossa bradanica.

INTRODUCTION

The assessment of tectonic activity in low-relief sectors of young orogens is very difficult, since few methods are available, especially in areas characterized by low seismicity. In geomorphology, the recognition of tectonic landforms is supported by the computation of geomorphic indices, especially in gentle landscape. For example, drainage anomalies of fluvial systems that are not produced by lithology or climate changes, might show indicative geomorphic indices on very small ongoing topographic changes (Holbrook & Schumm, 1999). Most studies on the estimate of geomorphic parameters and indices come from areas affected by high-rate tectonic deformation (Bull & McFadden, 1977; Keller & *alii*, 1998; Azor & *alii*, 2002; Silva & *alii*, 2003; Harkins & *alii*, 2005; Soto & *alii*, 2005; Pérez-Peña & *alii*, 2010; Delcaillau & *alii*, 2011; Kirby & Whipple, 2012; Melosh & Keller, 2013; Demoulin & *alii*, 2015; Papanikolaou & *alii*, 2015; Martino & *alii*, 2017), whereas a few refer to regions of low-rate deformation (Pedrera & *alii*, 2009; Troiani & *alii*, 2014; Ntokos & *alii*, 2016; Matos & *alii*, 2016).

We investigated the eastern (i.e. external) sector of the southern Italian Apennines (fig. 1), bounding the foredeep. It belongs to the upper course of the Bradano River catchment basin and is characterized by two different landscapes: one, corresponding to the frontal imbricate fan structure of the chain, is formed of different sedimentary successions locally incised by well-developed fluvial valleys and shows a hilly relief; the other displays a low-relief and sub-planar areas corresponding to the Bradano Foredeep, composed of a relatively homogeneous cover of Pliocene-to-Pleistocene clastic deposits.

Compressive deformation of the frontal sector of the south-Apennine chain, as deduced by field evidence, is not younger than Middle Pleistocene (Schiattarella & *alii*, 2005), even if a recent and significant uplift of the whole area is suggested by geomorphological features. In this sense, we try to detect and discuss the meaning of the youngest landforms of the area with regard to the role of active tectonics in shaping the landscape of the chain front, by means of morphotectonic and morphometric analyses. To this scope, we analysed the distribution of fluvial terraces within the upstream of the Bradano River, the longitudinal profiles of fluvial terraces, the swath profiles across the frontal sector of the chain, and tectonically-sensitive geomorphic indices such as stream length-gradient index (SL), asymmetry factor (AF), sinuosity index (SI), and valley floor slope (VF_s).

GEOLOGICAL AND GEOMORPHOLOGICAL OUTLINES

The Tyrrhenian Sea, the southern Apennines, the Bradano Basin, and the Apulian plateau are the expressions of a single geodynamic system, representing respectively the back-arc basin, the orogenic chain, and its foredeep and foreland. The southern Apennines are an Adriatic-verging fold-and-thrust belt derived from the deformation of large Mesozoic–Cenozoic circum-Tethyan domains and associated Neogene–Pleistocene foredeep and satellite-basin deposits (Patacca & Scandone, 2007, and references therein). The tectonic units of the fold-and-thrust belt overlap the foreland deposits of the Apulian Platform. Starting from the Tortonian, the orogen underwent low-angle extension which led to the exhumation of its non-metamorphic "core complex" (Schiattarella & *alii*, 2006, and references therein). This regional frame has been extremely complicated by Quaternary tectonics, responsible for the segmentation of the chain and its uplift (Schiattarella & *alii*, 2017, and references therein).

The chain can be roughly divided into three zones, the inner, axial, and outer belts (numbered as 1, 2, and 3, respectively, in fig. 1), parallel to its NW-SE elongation axis. The inner belt corresponds to the Tyrrhenian side of the Apennines and its backbone is mainly composed of Mesozoic shallow-water carbonates and Cretaceous-to-Miocene deep-sea pelagic successions. The mountain range is transversally incised by fluvial valleys that drive the main rivers westward, toward the Tyrrhenian Sea, locally producing narrow gorges. Coastal ranges are alternated with graben-like structures generated by post-orogenic extensional faulting and filled with Pliocene-to-Quaternary sediments and volcanic products.

The axial belt is formed of Mesozoic-to-Cenozoic platform carbonate units thrust on the coeval deep-sea water pelagic units. Miocene flysch and clastic deposits of Pliocene thrust-top basins, both involved in contractional deformation, unconformably lie on these tectonic units. Quaternary extensional tectonics displaced the orogen and is still active along the axial zone of the chain (Schiattarella & *alii*, 2006, 2017; Barchi & *alii*, 2007; Martino & *alii*, 2009). Many mountain tops of the axial belt correspond to the remnants of Pliocene-Pleistocene erosional land surfaces uplifted and dismembered by Quaternary faults (Schiattarella & *alii*, 2013). The landscape of the axial zone includes block-faulted ridges and massifs bounded by high-angle fault scarps retreated by slope replacement processes (Giano & Schiattarella, 2014, and references therein) that were re-activated by active faults (Giano & *alii*, 2018). Tectonically-controlled intermontane basins filled with Pliocene-to-Quaternary fluvial and lacustrine deposits (Giano & *alii*, 2014) are also presents. The fluvial networks follow the strike of the structures and often transversally cut the bedrock to flow into the Tyrrhenian, Adriatic, or Ionian seas.

The outer belt of the chain is made of Cenozoic sandstones, marls, and clay forming the eastern imbricate fan of the orogenic wedge. Its front tectonically overlap the Pliocene-Pleistocene clastic deposits of the Bradano Foredeep or is locally buried by such sediments. The outer belt is characterized by a lack of extensional block-faulting and a general passive north-eastward tilting as a consequence of the uplift of the chain. This is also supported by the major rivers that often flow perpendicularly or obliquely to the elongation of the main tectonic structures. Such an uplift produced the progressive emersion of the Bradano Foredeep (Casnedi, 1988) and the establishment of the hydrographic network (Corrado & *alii*, 2017). The outer belt displays a landscape with an average elevation lower than the axial belt.

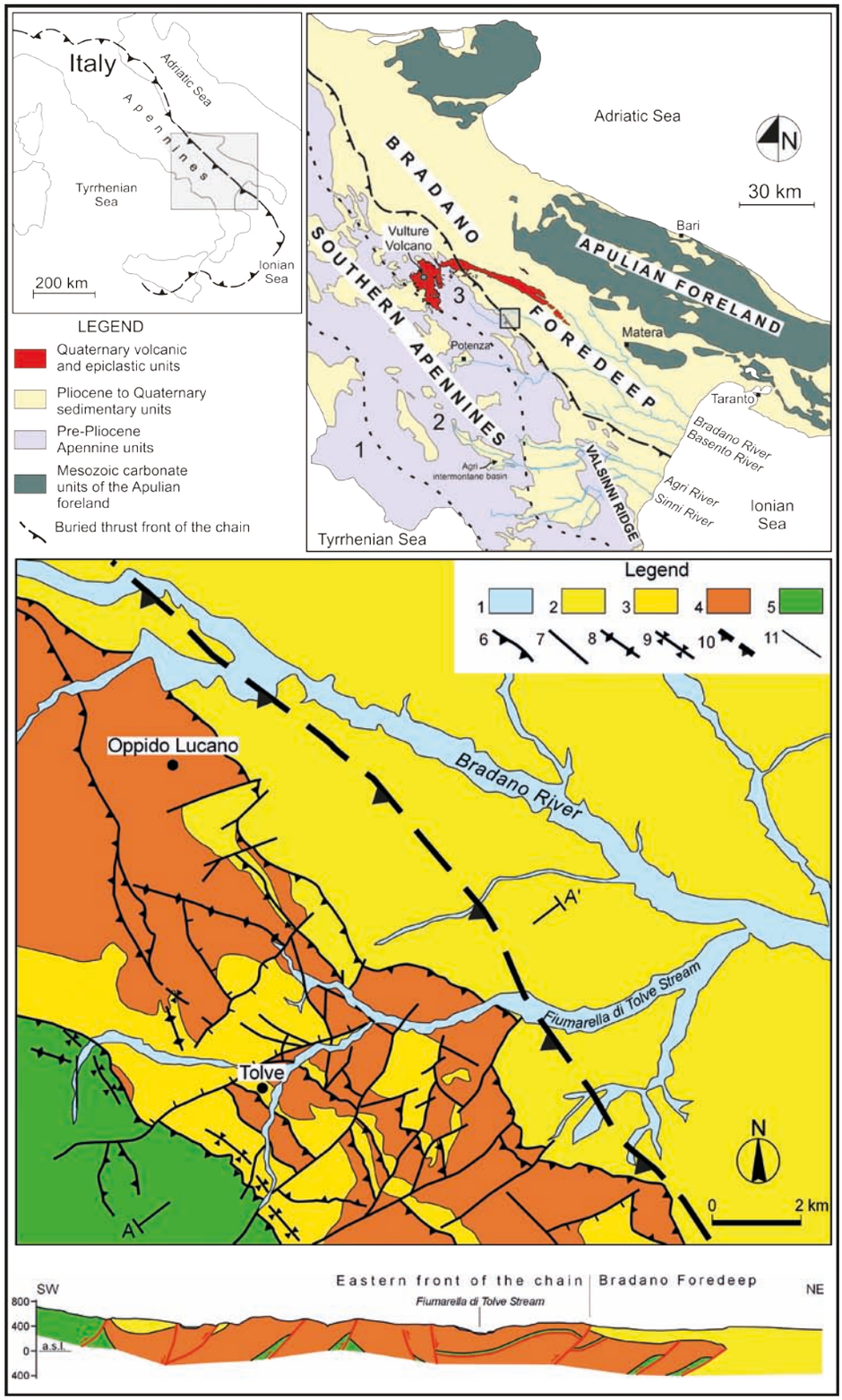

FIG. 1 - (A) Geological sketch map of the southern Apennines (study area in the small grey box); dashed lines separate different morphostructural belts of the orogenic chain (1: inner or Tyrrhenian belt, 2: axial zone; 3: outer or external belt, coinciding with the eastern thrust imbricate fan). (B) Geological sketch map of the study area. Legend: 1) Holocene alluvial deposits; 2) Pliocene-to-Quaternary clastic deposits of the Bradano foredeep; 3) Pliocene-to-Pleistocene deposits of the thrust-top basins of the chain; 4) Miocene siliciclastic deposits of the outer belt; 5) Cretaceous to Miocene units of the chain; 6) thrust; 7) high-angle fault; 8) anticlinal axis; 9) synclinal axis; 10) buried thrust front of the chain; 11) stratigraphic boundary. (C) Cross-section through the external belt.

Pliocene-to-Pleistocene sedimentary infill of the Bradano Foredeep is constituted by a transgressive-regressive clastic sequence of conglomerate, sand, and clay. Middle-to-Late Pleistocene fluvial terraces are distributed along the valley sides of the Bradano River, and both Holocene slope deposits and landslides are scattered in the whole study area.

The study area is placed between the frontal portion of the outer belt of the chain and the Bradano Foredeep and, therefore, shows marked differences in topography. In fact, it is characterized by a hilly landscape with a topography that varies in elevation from 900 m a.s.l. of the western watershed of the Fiumarella di Tolve Stream to 200 m a.s.l. of the Bradano River floodplain (fig. 1). Different main types of landforms characterize the study area: i) flat-topped highs representing remnants of older erosion surfaces and lower fluvial terraces vertically incised by the Bradano River and its tributaries; ii) wide or narrow V-shaped fluvial valleys, generally NW-SE- and NE-SW-oriented; iii) few dozen meters high steep slopes or vertical scarps that bound the edges of both flat erosion surfaces and fluvial terraces; iv) horizontal, generally elongated, river floodplains. All these landforms pertain to two different major landscape units, roughly separated by the trace of the buried frontal thrust (figs. 1 and 2) coinciding with the border between the frontal part of the allochthonous wedge and the adjacent foredeep.

The NW-SE-striking buried thrust front of the chain, so as inferred by geological and geophysical explorations, and the main associated surficial breaching thrusts are reported on the sketch map of figure 1. These latter structures produced anticlinal and synclinal folds which were cut by high-angle strike-slip faults active since the Lower Pleistocene (Pieri & *alii*, 2011). In the Vulture Volcano area, not far from the study area and also located in the outer belt of the chain, the existence of transpressional structures sutured by a palaeosol overlaid by a 484±8 ka B.P. unit indicates that such a frontal zone underwent a NE-SW contraction even during the middle Pleistocene (Schiattarella & *alii*, 2005). No field evidence of Late Pleistocene to Holocene tectonic activity has been found in the study area and information coming from the seismicity are evenly scarce. The study area is far from the seismically active sector of the southern Apennines and is included within the zone 2 of the Seismic Zonation Map of Italy, with a peak ground acceleration of 0.25 g (downloaded at: www.ingv.it). In fact, the spatial distribution of earthquakes with magnitude M>2 starting from 1900 AD to present is mainly concentrated in the axial zone of the belt (fig. 2) and this means that the studied sector is currently affected by a low-rate deformation. However, we observe at least a dozen earthquakes of different magnitude and depth that could suggest a probable tectonic activity of the area. The location of earthquake epicentres in the study area is placed

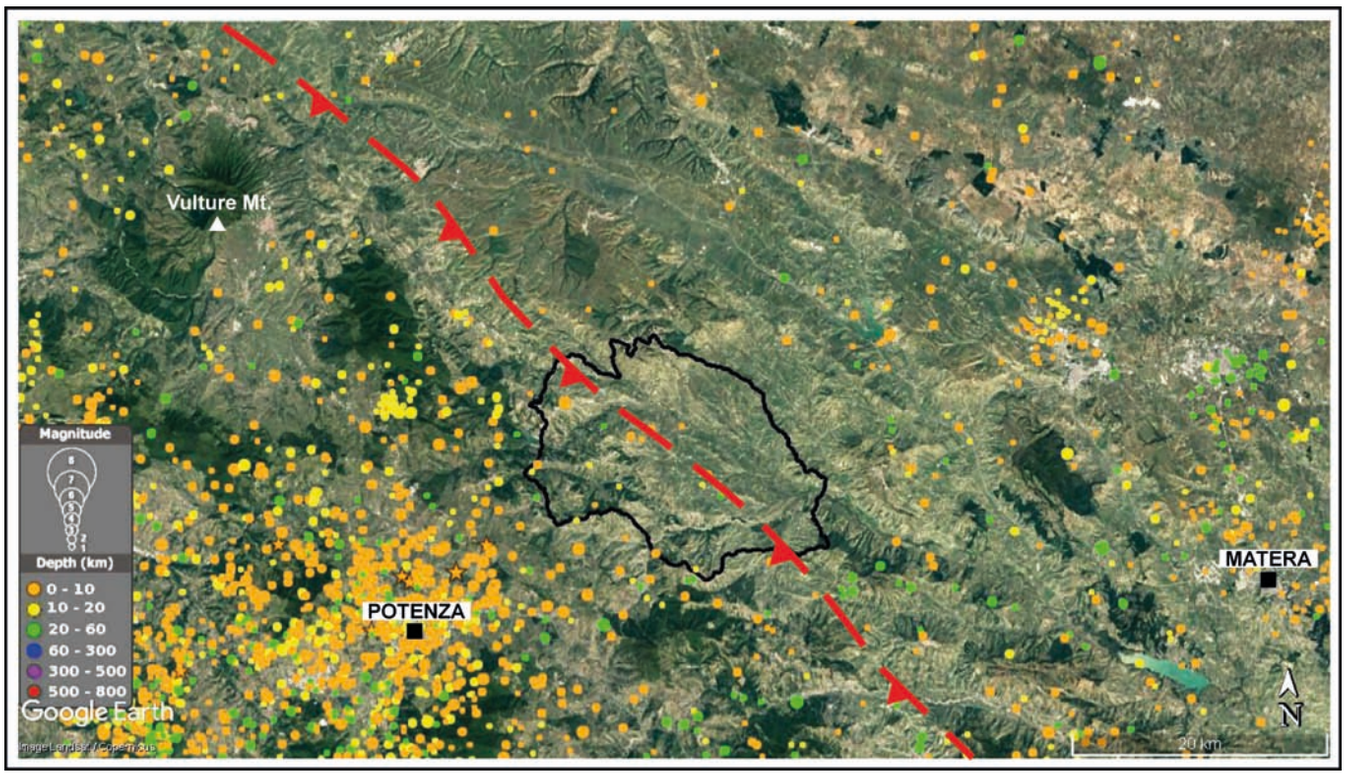

FIG. 2 - Spatial distribution of earthquakes in the study area and surroundings, with magnitude and depth of hypocentres M>2. Circles reported on the map are the hypocentres of earthquakes collected within a range from 1900 AD to Present. Data were extracted from the Italian Seismological Instrumental and Parametric Data-Base (ISIDe, http://iside.rm.ingv.it).

along a narrow belt roughly parallel to the NW-SE-trending buried thrust front of the chain, whilst no epicentres are in the left-side valley of the Bradano River (fig. 2). If we can exclude or minimize the role of the control of lithology and climate on that area, any morphological variations of the valley floor and the longitudinal channel profile of the Bradano River could be related to tectonic activity of blind structures.

METHODS

Geomorphological data coming from different approaches, such as field surveys, aerial photo interpretation, DEM-based elaboration, and fluvial terrace analysis, have been used here to provide results on the behaviour of the frontal thrust zone of the Lucanian Apennine segment. Both field data and aerial photo interpretation have been collected in a geographical information system.

Pleistocene fluvial terraces are arranged on both sides of the Bradano River valley. Besides their spatial distribution, the longitudinal profiles of these terraces have been analysed in comparison with that of the present-day Bradano River valley. Furthermore, three NE-SW-oriented swath profiles showing the maximum, mean, and minimum elevation a.s.l. of the whole study area have been extracted from a 20 m-resolution DEM free downloaded at http://www.pcn.minambiente.it. Topographic features influenced by tectonic activity have also been taken into account by using several geomorphic indices based on the analysis of drainage networks. Tectonically sensitive morphometric parameters have been extracted from the same 20 m-resolution DEM using the ArcGIS® software, such as the stream length-gradient index (SL), the asymmetrical factor (AF), the sinuosity index (SI), and the valley-floor slope (VF_s). In particular, these indices may detect anomalies in the landscape features produced by local changes in tectonic activity resulting from an uplift or subsidence (El Hamdouni & *alii*, 2008).

Geomorphic indices

The stream length-gradient Index (SL index) earlier developed by Hack (1973) may be calculated along a longitudinal stream profile and used to evaluate the erosional resistance of the involved rocks and the relative intensity of active tectonics (Azor & *alii*, 2002; Font & *alii*, 2010). It is very sensitive to measure minimal changes or variations in the channel slope, thus furnishing useful information on tectonic activity (Burbank & Anderson, 2001; Keller & Pinter, 2002; Troiani & Della Seta, 2008). SL index is normally associated to stream power (Perez-Pena & *alii*, 2009) and presents high values in areas where rivers cross hard resistant rocks or tectonics is still active, and low values where cross soft resistant rock or tectonics is weak (Merritts & Vincent, 1989; Azor & *alii*, 2002; Keller & Pinter, 2002; Chen & *alii*, 2003; Troiani & Della Seta, 2008). The SL index is defined as:

$$SL = (\Delta H/\Delta L)\times L$$

where $\Delta H/\Delta L$ is the local slope, or gradient, of the channel reach, and L is the channel length from the divide to the midpoint of the channel reach. Comparison of the SL index along different stream-length segments is very difficult, because they are directly influenced by channel slope changes. To overcome this problem, many authors have used the graded river gradient K as a normalization factor (Seeber & Gornitz, 1983; Chen & *alii*, 2003; Pérez-Peña & *alii*, 2009). In this work, SL_k values have been reported on a SL_k map following the method proposed by Perez-Pena & *alii* (2009) that allowed us to detect the trending anomalous areas related to different rocks and faults thus discriminating their lithological or tectonic meaning. According to Perez-Pena & *alii* (2009), to avoid relevant errors in the computation of the SL_k index, we have chosen a linear channel reach of 40 m considering the 20 m-resolution of the DEM. Furthermore, the drainage network has been manually digitized based on the 1:25.000 contour map edited by the Italian Geographical Military Institut (IGMI).

SL_k values distributed in the map as points (fig. 3a) are then interpolated using the Inverse Distance Weighting technique (IDW), by search radius parameter, from the Raster Interpolation toolset of ArcGIS®. As a result, a spatial distribution of 1st to 3rd order basins was carried out. The best results from IDW technique are obtained when sampling is sufficiently dense with regard to the local variation one is attempting to simulate. If the sampling of input points is sparse or uneven, results may not sufficiently represent the desired surface (Watson & Philip, 1985). The presence of few points scattered in the 1st order basins produced an incorrect statistical analysis and then not considered in the elaboration. Also the 2nd order-based analysis did not produce appreciable results. To solve this discrepancy the basins area lacking of data has been deleted using the mask tool of ArcGIS®, thus obtaining only the 3rd order basins distribution with few errors (fig. 3a). According to Beneduce & *alii* (2004) and Capolongo & *alii* (2005) these basin orders are sufficiently young and receptive of active tectonic deformation.

The asymmetry factor (AF) illustrated by Keller & Pinter (2002) is a parameter used to evaluate tilting at drainage basin or mountain front scale in response to tectonic activity or lithological control (Hare & Gardner, 1985; Keller & Pinter, 2002) using the following equation:

$$AF = (Ar/At)\times 100$$

where A_r is the area of the basin to the right (facing downstream) of the trunk stream and A_t is the total drainage basin area. The AF index is very sensitive to tilting occurred perpendicular to the channel direction and results close to 50 in a basin developed with little or no tectonic activity. The AF index above or below 50 may suggest a tilting of the basin roughly orthogonal to the main trunk stream.

Sinuosity is a property of a channel stream to change its course from a straight to a meander drainage line. It may be expressed as the ratio between the distance covered by meanders and the straight line distance covered by the same meanders (Schumm, 1977; Keller & Pinter, 2002) as follows:

$$SI = Lc/Lv$$

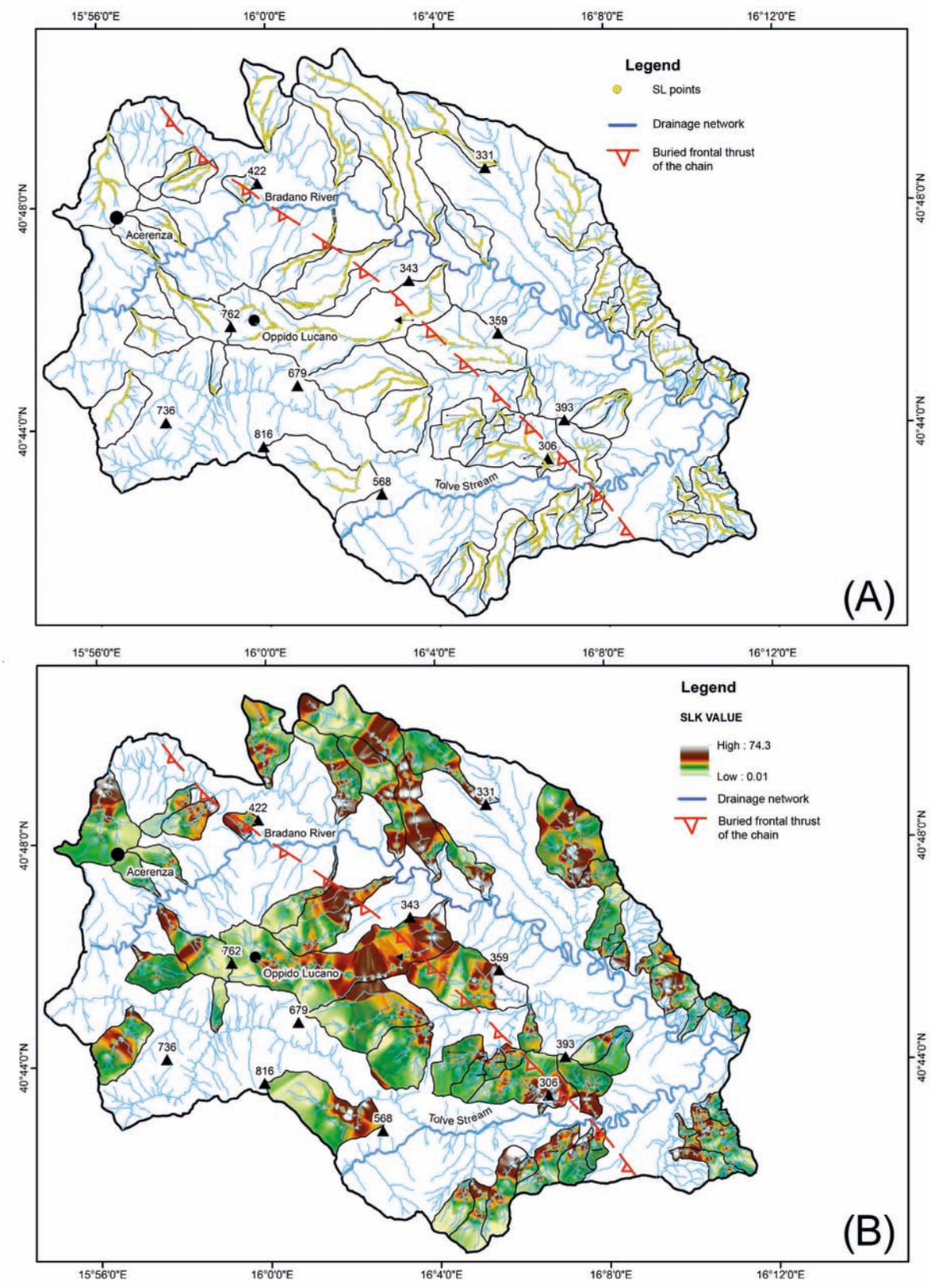

FIG. 3 - Distribution of SL points used to measure the SL index (A), and distribution map of SL_k values in the study area (B). The latter map was extracted using a mask in ArcGIS by a SL_k map of the whole study area.

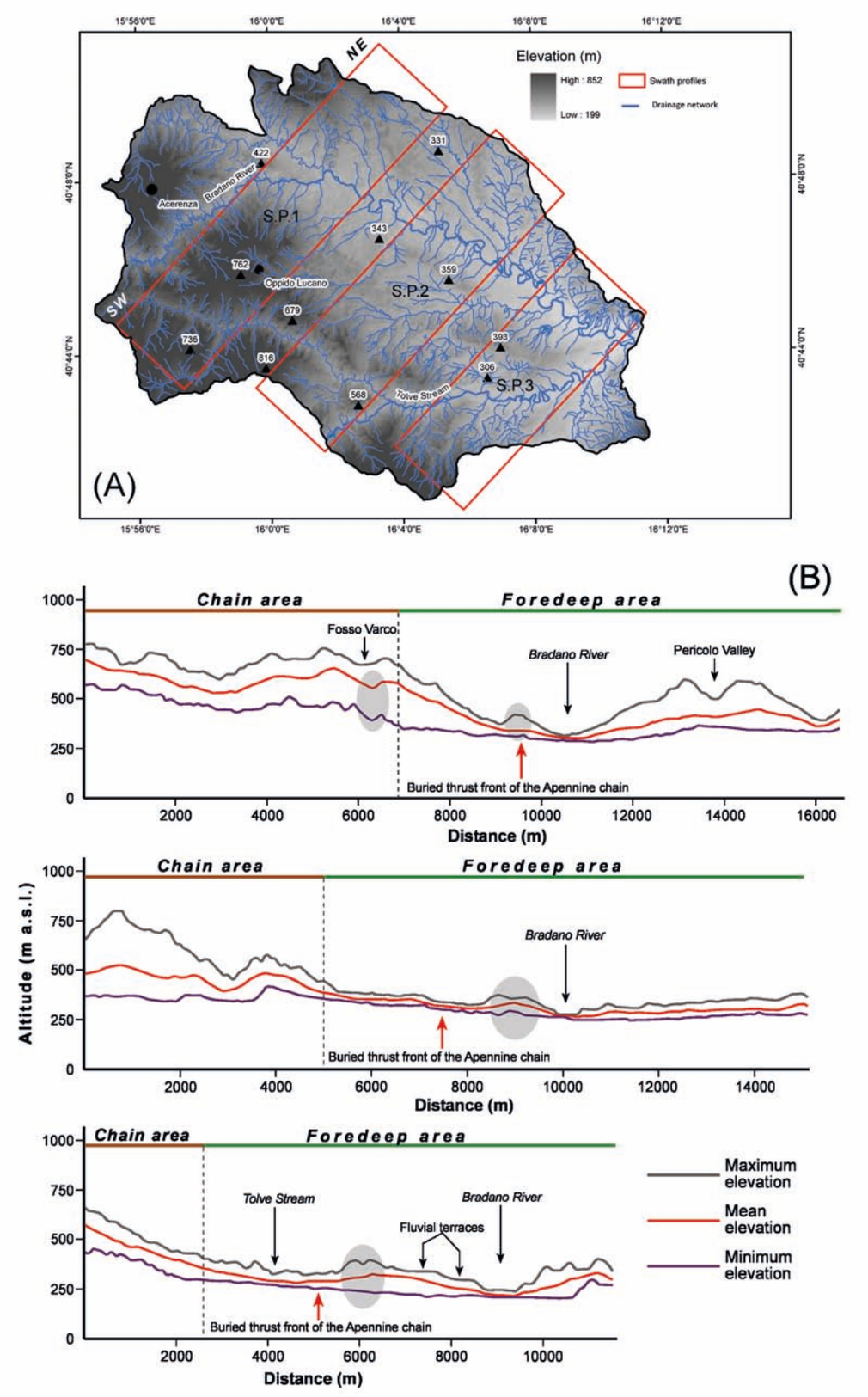

FIG. 4 - Red lines in the map indicating the boxes used to compute the three swath profiles (A); swath profiles across the thrust front of the chain and adjacent foredeep (B), grey ellipses show the topographic anomalies recognized on each profile.

Where L_c is the channel length measured along the centre of the channel and L_v is the valley length measured along the valley axis. SI value ranges from <1.1 for completely straight channels, to 1.1-1.5 for meandering channels, up to >1.5 for highly tortuous river channels. Variations of SI index are mainly controlled by water discharge and sediment loading that vary in response to tectonic, climate, and anthropogenic factors (Schumm, 1977). Sinuosity index was largely used to investigate the amount of the vertical deformation on channel rivers in tectonically active areas (Ouchi, 1985; Keller & Pinter, 2002; Holbrook & Schumm, 1999) assuming that if such deformation persists for only few decades the displacements achieved will be sufficient to generate significant changes in channel morphology. The deflection of rivers around an uplifted area or into a zone of subsidence will be manifested as an abrupt shift in the river courses sinuosity corresponding to the deformed zone (Holbrook & Schumm, 1999).

Further, we also used the valley-floor slope (VF_s) parameter which represents the gradient of the modern channel longitudinal profile measured along different selected reaches of river, particularly where the changing slope is influenced by tectonics (*sensu* Schumm, 1986). In the study area, the Bradano River profile has been segmented into upper, middle and lower reaches.

Morphotectonic markers

The arrangement of fluvial terraces has been widely used as a morphotectonic marker in many geological settings (Wells & *alii*, 1988; Merrits & Vincent, 1989; Giano & Giannandrea, 2014). Remote sensing of river terraces allowed us to create a relative landform hierarchy. A field evaluation is also required to confirm or refine the location and numbers of river terrace levels, thus permitting mapping, valley cross-sections, and plotting in height range diagrams (Stokes & *alii*, 2012) different terrace levels against the modern river longitudinal profiles. Fluvial terraces of the study area have been recognized by using aerial photo interpretation and mapped in a field survey on a 1:25000 contour map of the I.G.M.I.; the modern longitudinal profile of the Bradano River channel has been instead extracted from a 20 m-resolution DEM and plotted against the fluvial terraces profiles so as to compare their slopes. The aim is to obtain a diverging or converging downstream gradient slope (*sensu* Pierce & Morgan, 1992) with regard to the modern river channel profile, that could be interpreted as a passive response induced by a rapid uplift (Burbank & Anderson, 2001; Giano & Giannandrea, 2014).

Swath profiles are a useful way to characterize the dynamic topography of orogenic belts where along-strike

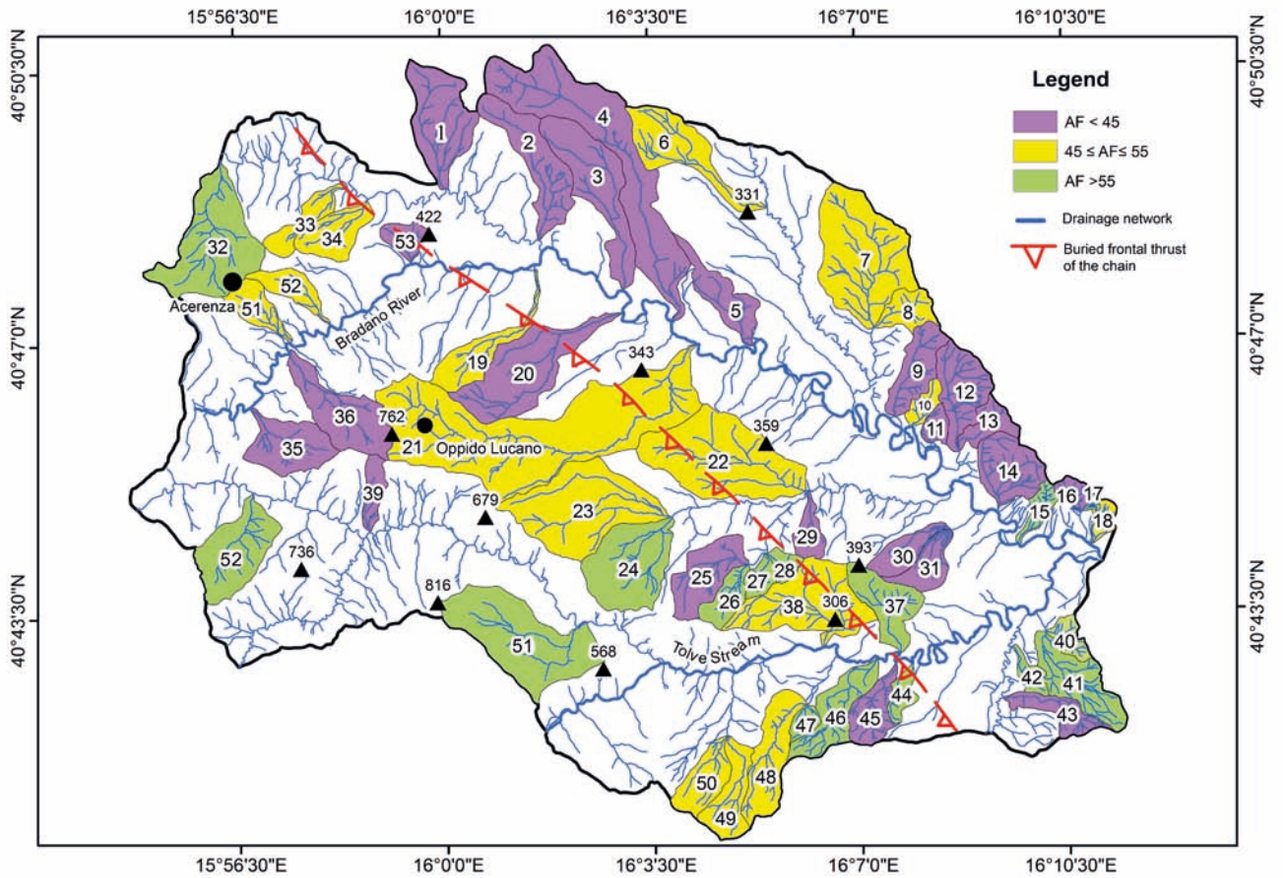

FIG. 5 - Map of the AF values of the study area. Values of AF<45 indicate a left-tilting basins, values of AF>55 indicate a right-tilting basins, whereas no tilting corresponds to 45≤AF≤55 values. Progressive numbers indicate the different drainage basins discussed in the text.

variations are small and areas are tectonically active, using variation in the maximum, minimum, and mean elevation ranges (Isacks, 1992). The technique uses a topographic profile taken perpendicularly to the strike of the structures and all max, min, and mean elevations within a defined width are projected into the plane of the profile. For topography with a few isolated peaks the average curve will be close to the minimum whereas for recently incised regions with a few major rivers the average curve will be close to the maximum (Masek & *alii*, 1994). Difference between the maximum and minimum envelopes represents a measure of local relief at length scales of the order of swath width. Three NE-SW-oriented swath topographic profiles have been created in the study area, orthogonally to the strike of the buried thrust front of the chain (fig. 4a). All the profiles are 4 km wide and they have been generated by sampling elevation values along 100 m-spaced parallel lines, which appeared as satisfactory for the issues faced in this work.

RESULTS

The spatial distribution of earhquakes with magnitude M>2 (fig. 2) suggests that the study area underwent low-rate deformation. A dozen of low-magnitude earthquakes are scattered along a narrow belt roughly parallel to the NW-SW-trending buried thrust front of the chain, exclusively in the right-side valley of the Bradano River. In this work, the SL_k map was used to detect anomalous areas related to different rocks and faults thus discriminating their lithological or tectonic meaning. The peak values of the SL_k related to 3rd order basins (fig. 3b) are scattered in the western sector of the area close to the Acerenza village, whereas more continue values are found east to the Oppido Lucano village, in the central sector of the study area. Relevant peak values are in the north-eastern sector of the left-side valley of the Bradano River showing an arrangement in a NW-SE-trending. An ENE-WSW trend of peak values is present on the right-side of the Tolve Stream, whereas peaks are placed around two top mountains at 568 m and 306 m a.s.l., respectively (fig. 3b) in the left-side valley.

The AF values, grouped into three classes discriminated by coloured areas (fig. 5), indicate the possible tilt direction of basins. First class includes the 45≤AF≤55 values suggesting no tilting (yellow basins in fig. 5), second class contains the AF<45 values indicating a left-tilting basin (purple basins in fig. 5) whereas third class is formed by the AF>55 values indicating a right-tilting basin (green basins in fig. 5). The spatial distribution of AF values shows that they are arranged in clouds corresponding to a certain number of basins, such as basins from 1 to 5 in the north-eastern side of Bradano River, and those from 19 to 23 in the central sector of the study area. Basins included in clouds with similar AF values are grouped in 9 clusters of basins spread on the entire area (tab. 1). Moreover, few isolated basins do not fall in any clusters.

The sinuosity index (SI) computed for different fluvial reaches of both the Bradano River and Tolve Stream shows similar patterns in terms of wave length and amplitude of meanders (fig. 6). The NE-SW-oriented upstream reach (A) of the Bradano River has a 1.4 value corresponding to a low meandering channel; both the B and C reaches are NW-SE-oriented and show values of 2.5 and 2.9, respectively, indicating well-developed meanders. Also the Tolve Stream shows three channel segments with different SI values: both the D and F reaches have a value of 1.2, whereas the segment E is featured by a value of 2.1 related to well-developed meanders.

The Valley-floor slope (VF_s), measured on three different reaches of the Bradano River valley, show a high value in the upstream course A (fig. 6), flowing in a NE-SW direction. Its VF_s percentage value of 1.19% is greater than those of the middle B and lower C reaches (fig. 6), both flowing in a NW-SE direction, respectively at 0.34% and 0.65%. VF_s values of the Tolve Stream show quite similar percentages in the upstream reach D (1.31%) and in the middle one E (1.10%), whilst a lower value (0.64%) is recorded in the reach F (fig. 6).

Three NE-SW-oriented swath topographic profiles have been developed in the study area and are here used to describe the anomalies observed among the max, min, and mean elevations. On the three transect we can identify two anomaly points along the northernmost swath profile and one for the two others (grey ellipses in fig. 4b). The anomaly points may reflect uplift-induced increase of the topography (fig. 4b).

Three orders of unpaired fluvial terraces distributed along the fluvial valleys of both the Bradano River and Tolve Stream has been recognized (fig. 7a). The first and highest fluvial terrace (T1) crops out on both the right- and left-side of the Bradano valley, at about 310 to 390 m a.s.l.; the second order terrace (T2) is well developed only along the right-side valley of Bradano River, from about 240 to 333 m a.s.l.; the third and lowest terrace (T3) is mainly present on the right-side valley, starting from the confluence of Tolve Stream and Bradano River toward NW.

INTERPRETATION AND DISCUSSION

Fluvial geomorphometry

SL_k peak values related to 3rd order basins (fig. 3b) roughly follow a spatial correlation along a NW-SE-directed trend, on both the left and right valley sides of the Bradano River. This means that SL_k anomalies of the study area are strictly controlled by tectonic activity of the buried thrust front. Rare high values from the western portion of the map could be associated to differential erosion rather than tectonics. In fact, lithology seems to be a control factor of SL_k peak spots, so as in the case of the basins 32 and 34 (cf. figs. 3b and 5) in which the shift from high to low values is due to the sharp contact between conglomerate and clayey deposits. More in general, this arrangement from more to less resistant rocks occurs in the transition from a pre-Pliocene marly bedrock to Pliocene clastic successions (basin 32, cf. figs. 3b and 5), from Miocene clayey-marly to arenaceous formations or from Pleistocene clay to Miocene sandstone (basins 21 and 48, respectively, cf. figs. 3b

TABLE 1. Drainage basins grouped by AF values.

Left side			Right side		
Group	*Basin number*	*AF value*	*Group*	*Basin number*	*AF Value*
A	1,2,3,4,5	<45	D	33,34,51,52	45<AF<55
B	6,7,8	45<AF<55	E	35,36,39	<45
C	9,11,12,13,14,16	>55	F	19,21,22,23	45<AF<55
			G	26,27,28	>55
			H	48,49,50	45<AF<55
			I	40,41,42	>55

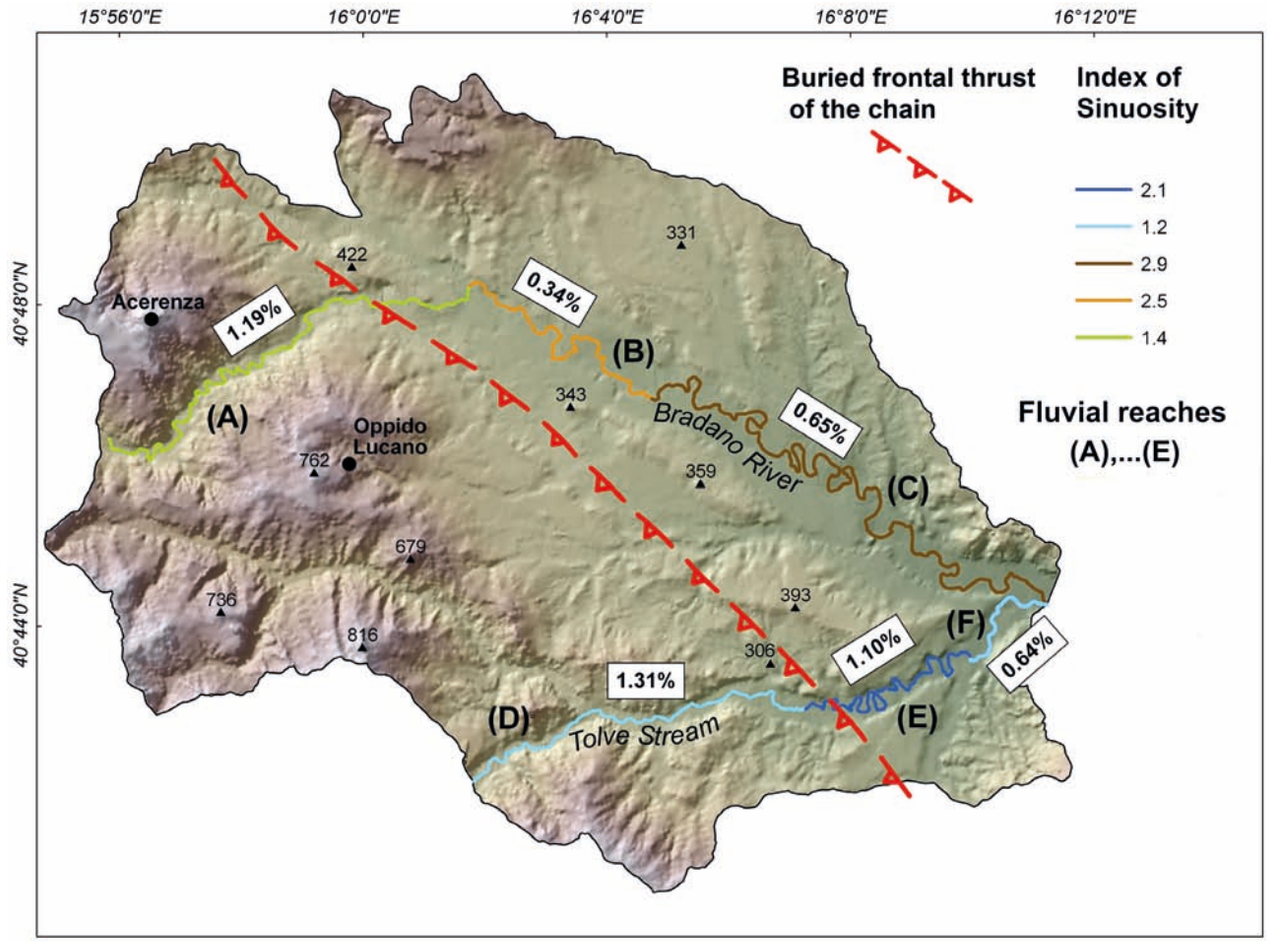

FIG. 6 - Map showing the sinuosity indices (SI) and valley floor slope (VF_s) of major rivers of the study area.

and 5). On the contrary, basins 35 and 36 - located in the right-side valley of the Bradano River, don't show differences in lithology and then their anomalies may be attributed to tectonics, as also suggested by the AF index values (fig. 5).

The north-eastern sector of the study area mainly features clay deposits and the SL_k anomalies may be entirely attributed to tectonics, except for the upstream of some basins where a transition from sandy to clayey successions occurs. Although selective control of lithology seems to be well represented in the study area, tectonics appears to be the dominant factor in controlling the morpho-evolution. SL_k anomaly values are clustered following the NW-SE "Apennines chain" orientation, and are well displayed where no lithological variation have been observed. Considering the same orientation of both the SL_k anomaly clus-

ters alignment and buried thrust front, it could be possible to associate the origin of SL_k anomalies to the recent tectonic activity of such a structure.

In the left side of Bradano River, three groups of AF values are recognized (A, B, and C in tab. 1). Both A and C groups show AF values <45 indicating a left tilting of basins, and only the B group has neutral values suggesting no tilting. In the right side of Bradano River, six groups of basins are found (D, E, F, G, H, and I in tab. 1). Three of them (D, F, and H groups) with values 45<AF<55 indicate a substantial tectonic stability, whereas G and I groups have a value of AF>55, and only the E group has a value of AF<45. Furthermore, single basins that are mainly scattered in the right side of Bradano River show values of the AF index changing from <45 to >55. These latter values related to the single basins seem to be mainly controlled by lithology instead of tectonics. As shown in figure 8, the three groups of AF values are widely scattered in the whole right side of Bradano River valley, and although AF values <45 are few abundant with regard to values >50, they are casually distributed and do not show a main tilting direction. On the left side of Bradano River valley, the values of AF<45 are well distributed in the A and B groups of basins and are more abundant than the neutral values. This condition suggests that a south-westward tilting of the area could be considered in the left side of the major valley. Due to the lithological homogeneity of the left side of that valley, shaped in clay and sands, we can conclude that the anomalies of AF values are induced by recent tectonic activity.

Variation of the sinuosity index is mainly controlled by sediment yields and related climate but can also be caused by recent tectonic uplift (*sensu* Holbrook & Schumm, 1999). An abrupt increase of SI values could be assigned to a recent local uplift of the area produced by tectonic activity. SI index was measured in the Bradano River and Tolve Stream, two well-developed meandering rivers (fig. 6), established in the early continental stage of the catchment area. In this sense, they have produced a very sensitive channel pattern in the floodplain (Holbrook & Schumm, 1999; Ouchi, 1985). The NE-SW-oriented upstream reach (A) showing a low SI value produces a sharp deflection of its course toward the NW-SW direction. The inlet of the Fiumarella Stream, a tributary of the Bradano River flowing in the NW-SE direction, marks the change of the SI value from (A) to (B) reaches. Such a tributary produces an increase of the water flow discharge in the Bradano fluvial channel and – together with the sharp decrease of the fluvial slope gradient – is responsible for the formation of a braided-like configuration of the channel reach B. The reach C, conversely, shows a meandering belt and high SI values from 2.5 to 2.9. SI distribution in the Tolve Stream shows high values of 2.1 thus suggesting an uplift occurred both in upstream and downstream sectors (fig. 6). The general increase of SI could be explained as a consequence of tectonic activity that produced a tilting of the whole area toward the south-east.

Valley-floor slope (VF_s) values, measured on three different reaches of both the Bradano River and Tolve Stream, show low percentages because of the hilly landscape of the area and its lithological nature (clay, sand, and conglomerate deposits), easy to erode by surface processes. In the Bradano river valley, the VF_s value of the reach A is up to 3 times greater than the reach B and almost twice the reach C, while this latter value is almost twice the reach B. This discrepancy reveals the existence of break points in the valley slope probably due to a weak bending of the area that could be explained as the surface effect of an active buried thrust. Slope gradient of the Tolve Stream valley is upward concave both in D/E and E/F breaks: no information about tectonic activity can be achieved from such a configuration.

Other geomorphological evidence of tectonic activity

The three swath profiles cross cut orthogonally the NW-SE-directed imbricate fan and prosecute in the adjacent foredeep, including the whole upstream of Bradano River valley. As a rule, the mean elevation of the chain area is higher than the foredeep one (fig. 4b), due to a sharp change of lithology, passing from the chain harder rocks to more erodible formations of the foredeep. Nevertheless, some anomalies result as evident if we compare the three profiles of each single transect, where they diverge from a similar shape. In such a way, we can identify two anomaly points along the northernmost swath profile and one in the other two transects (grey ellipses in fig. 4b). Yet, on the left side of the Bradano valley, the consistent vertical incisions observed in the maximum elevations profile, corresponding to the Pericolo valley, seem to be related to lithological control. The persistent presence of buried active faults revealed by anomalies in the three swath profiles can be interpreted as blind thrusts, representing the propagation toward the foreland of the compressional deformation. It is worth noting that in the central swath profile the anomaly is located in the area where different orders of fluvial terraces crop out. In the southernmost swath, the chain area is less represented and the profile is quite entirely created in the foredeep area. The evident anomaly of the right side of the Bradano River valley is placed backward the fluvial terraces, promoted by the tectonic activity of the area. Conversely, the curve shape incongruence of the northeastern side of the swath profile seems to be correlated to lithological transitions from sandy to clay deposits. The analysis of the anomalies detected in the swath profiles are mainly imputable to the recent tectonic activity of the area and only in minor amount to lithological control. Such anomalies are located along a narrow belt parallel to the NW-SE-striking surficial trace of the imbricate fan and its frontal (partly buried) thrust, and distributed in a range of 3.5-6.5 km far away from the eastern mountain front of the southern Apennines, as already recognized by Riviello & *alii* (1997) and Labriola & *alii* (2008).

The three unpaired terraced developed along the Bradano River valley are labelled as T1, T2, and T3. T1 terrace is developed in length for about 3 km at the confluence of Tolve Stream and Bradano River. It is formed by conglomerate, sand and subordinately silt, reaching about 10 m in thickness, and shows depositional facies changing from alluvial fan to braided fluvial plain (Pieri & *alii*, 2011). T2 terrace is formed of about 15 m-thick succession of con-

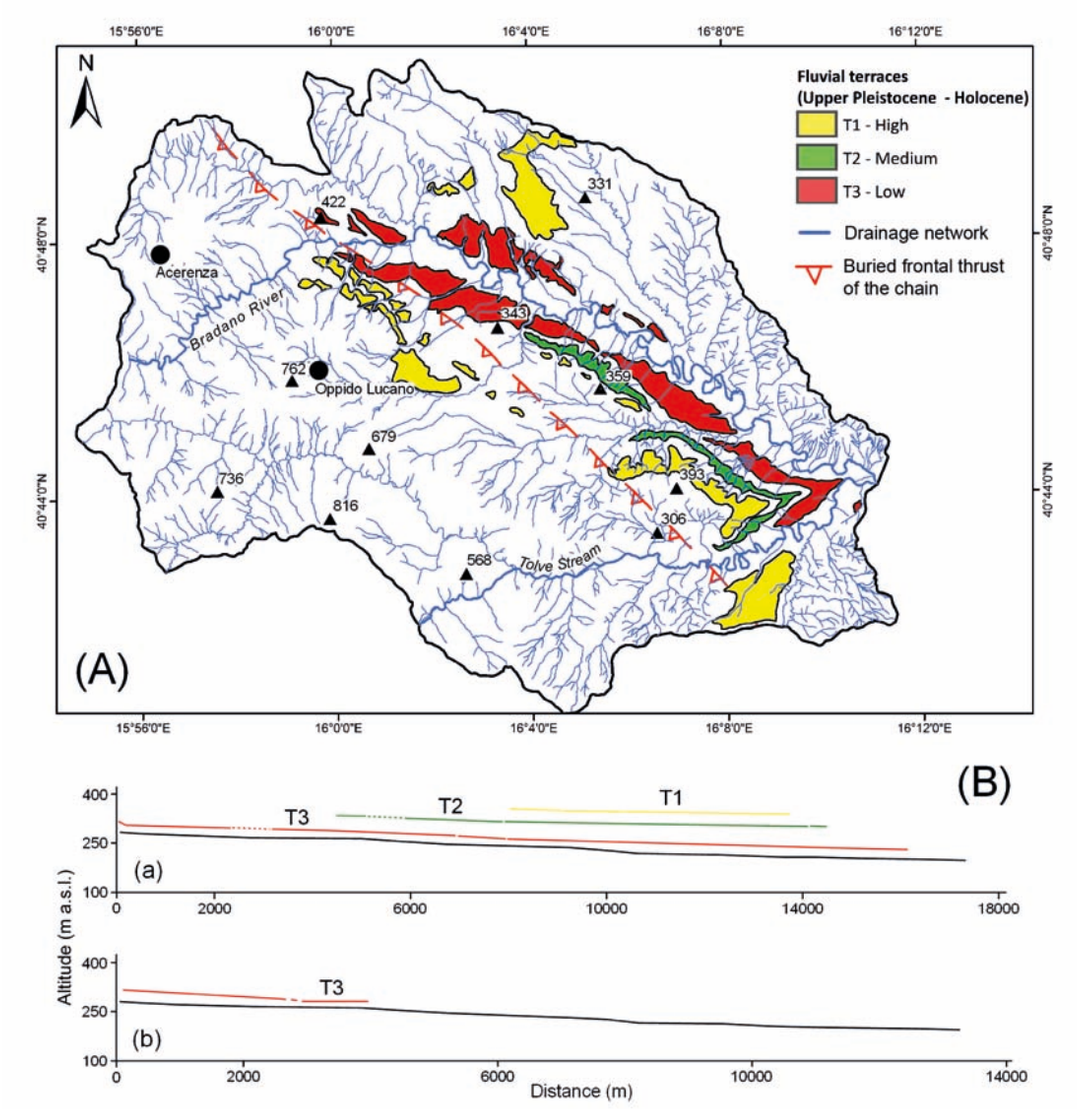

FIG. 7 - Geomorphological sketch map of the fluvial terraces of the Bradano River valley (A); Longitudinal channel profile of the Bradano River (black line) against T1, T2, and T3 longitudinal terrace profiles (yellow, green, and red lines, respectively), referred to right-side (a) and left-side (b) valley (B).

glomerate, sand, and silty sand, with depositional facies pertaining to both braided fluvial plain and alluvial fan (Pieri & *alii*, 2011). T3 terrace is formed of conglomerate and subordinately sand reaching a thickness of about 10 m. Their facies vary from alluvial fan deposits, located at the confluence of the main streams, to braided fluvial plain deposits distributed along the valley side (Pieri & *alii*, 2011). T1, T2, and T3 fluvial tread terraces partially coincide with the Middle to Late Pleistocene terraces recognized by Pieri & *alii* (2011).

Longitudinal channel profile of the Bradano River against T1, T2, and T3 longitudinal terrace profiles were plotted together (fig. 7b). Terraces profiles are parallel to the present-day Bradano channel profile, thus suggesting that no differential uplift (*sensu* Giano & Giannandrea, 2014) induced by the buried thrust occurred along strike at the chain front. Further, the unpaired terraces mainly distributed on the right-side of the Bradano River valley are indicative of a tilting toward NE of that part of foredeep, possibly due to the growth of the topography induced by tectonic activity (fig. 9).

CONCLUSIONS

The analysis of fluvial terraces arrangement and longitudinal profiles revealed that the study area underwent a diffused rising during the Late Pleistocene. In the Holocene, the same area seems to be affected by differential uplift due to tectonic tilting toward E-SE, resulting

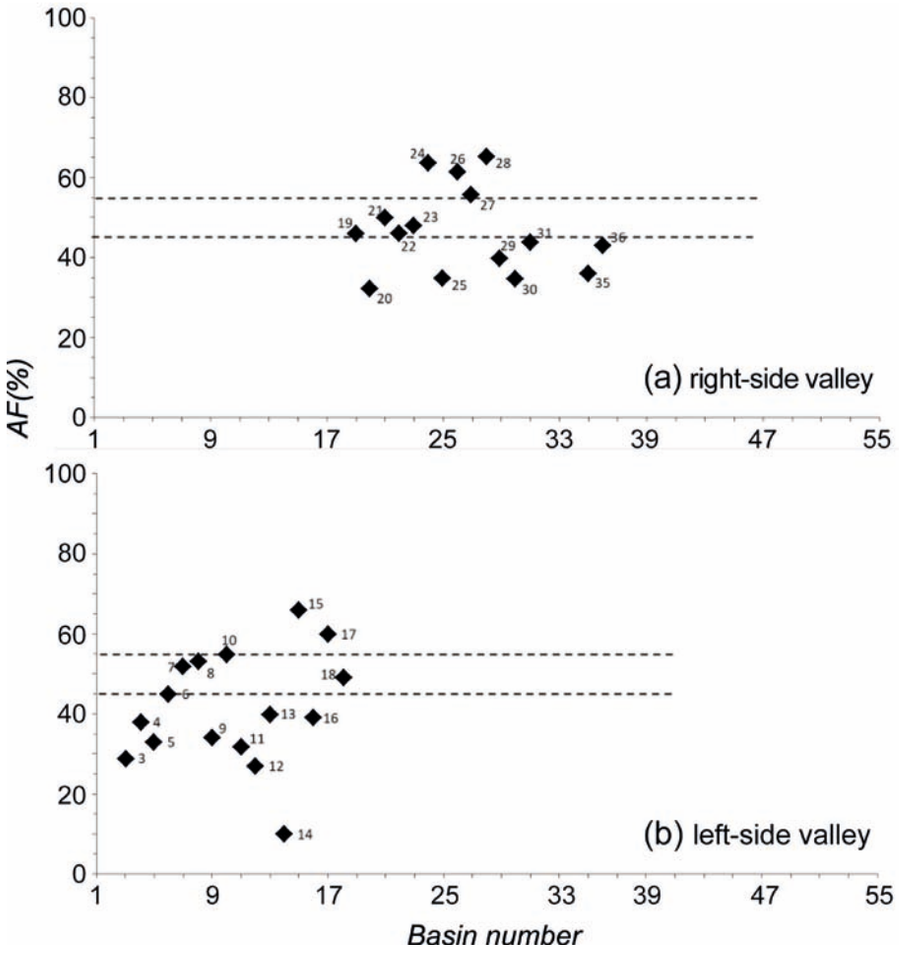

FIG. 8 - Scatter plots of the AF values related to both the right-side (a) and left-side (b) valley of the Bradano River. Dashed lines indicate the fields of existence of the AF values.

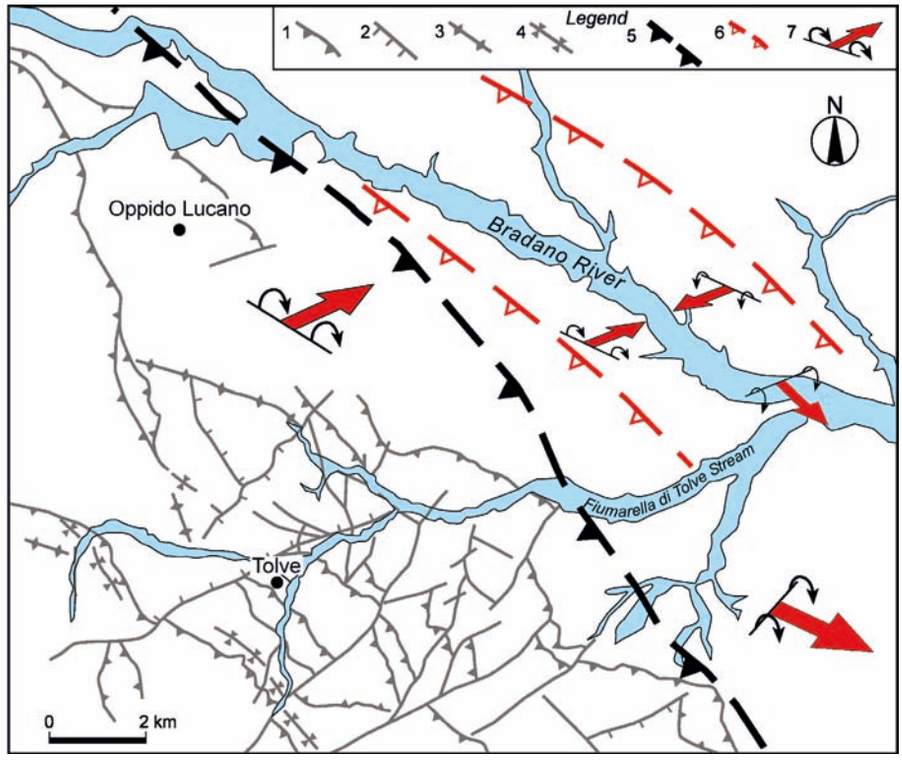

FIG. 9 - Map of tilting directions as deduced by geomorphic indices and fluvial terraces arrangement. Legend: 1) thrust; 2) high-angle fault; 3) anticlinal axis; 4) synclinal axis; 5) buried frontal thrust of the chain; 6) inferred blind thrust; 7) axis and direction of tilting.

from components toward NE and SE, as also supported by the increasing of the sinuosity index of the Bradano River. Tilting toward NE and SW is also detected by AF index and terraces pattern. It could be interpreted as a second-order effect due to topographic growth by blind thrusting.

Tectonic mobility has been adequately proved by other indices such as the asymmetry index and the stream length-gradient index. The mapping of the SL_k values has also shown that the anomalies follow NW-SE trends, suggesting a very recent tectonic activity of buried structures. Similar results have been obtained by swath profile analysis, with peaks in coincidence of the main outcropping thrust and of more external buried structures located in the foredeep.

In conclusion, geomorphic data and parameters led to consider the frontal portion of the Lucanian Apennine as still tectonically active, though its recent evolution has not been uniform in space and time. If the tectonic activity has to be relate to thrusting, then the lack of relevant earthquakes may be due to generalized mechanisms of aseismic creep. Alternatively, uplift and tilting could be even linked to the gravitative displacement of the chain front induced by passive sinking and roll-back of the lower plate (i.e. the Apulian platform).

REFERENCES

Azor A., Keller E.A. & Yeats R.S. (2002) - *Geomorphic indicators of active fold growth: South Mountain-Oak Ridge anticline, Ventura basin, southern California*. Geological Society of America Bulletin, 114, 745-753.

Barchi M., Amato A., Cippitelli G., Merlini S. & Montone P. (2007) - *Extensional tectonics and seismicity in the axial zone of the southern Apennines*. Bollettino della Società Geologica Italiana/ Italian Journal of Geosciences, 7, 47-56.

Beneduce P., Festa V., Francioso R., M. Schiattarella M. & Tropeano M. (2004) - *Conflicting drainage patterns in the Matera Horst Area, southern Italy*. Physics and Chemistry of the Earth, 29, 717-724.

Bull W.B. & McFadden L.D. (1977) - *Tectonic geomorphology north and south of the Garlock fault, California*. In: Doehring D.C. (Ed.), *Geomorphology in Arid Regions*, Proceedings 8th Annual Geomorphology Symposium, State University of New York, Binghamton, NY, 115-137.

Burbank D.W. & Anderson R.S. (2001) - *Tectonic Geomorphology*. Blackwell Science, Oxford, 27 pp.

Capolongo D., Cecaro G., Giano S.I., Lazzari M. & Schiattarella M. (2005) - *Structural control on drainage pattern of the south-western side of the Agri River upper valley, southern Apennines, Italy*. Geografia Fisica e Dinamica Quaternaria, 28, 169-180.

Casnedi R. (1988) - *La fossa bradanica: origine, sedimentazione e migrazione*. Memorie della Società Geologica Italiana, 41, 439-448.

Chen C.Y., Sung Q. & Cheng K.Y. (2003) - *Along-strike variations of morphotectonic features in the Western Foothills of Taiwan: tectonic implications based on stream-gradient and hypsometric analysis*. Geomorphology, 56, 109-137.

Corrado G., Di Leo P., Giannandrea P. & Schiattarella M. (2017) - *Constraints on the dispersal of Mt. Vulture pyroclastic products: implications to mid-Pleistocene climate conditions in the foredeep domain of southern Italy*. Géomorphologie: Relief, Processus, Environnement, 23 (2), 171-182.

Delcaillau B., Amrhar M., Namous M., Laville E., Pedoja K., & Dugué O. (2011) - *Transpressional tectonics in the Marrakech High Atlas: insight by the geomorphic evolution of drainage basins*. Geomorphology, 134, 344-362.

Demoulin A., Beckers A., & Hubert-Ferrari A. (2015) - *Patterns of Quaternary uplift of the Corinth rift southern border (N Peloponnese, Greece) revealed by fluvial landscape morphometry*. Geomorphology, 246, 188-204.

El Hamdouni R., Irigaray C., Fernández T., Chacón J. & Keller E.A. (2008) - *Assessment of relative active tectonics, southwest border of the Sierra Nevada (southern Spain)*. Geomorphology, 96,150-173.

Font M., Amorese D. & Lagarde J.L. (2010) - *DEM and GIS analysis of the stream gradient index to evaluate effects of tectonics: The Normandy intraplate area (NW France)*. Geomorphology, 119, 172-180.

Giano S.I. & Giannandrea P. (2014) - *Late pleistocene differential uplift inferred from the analysis of fluvial terraces (Southern Apennines, Italy)*. Geomorphology, 217, 89-105.

Giano S.I., Gioia D. & Schiattarella M. (2014) - *Morphotectonic evolution of connected intermontane basins from the southern Apennines, Italy: the legacy of the pre-existing structurally controlled landscape*. Rendicondi Fisici Accademia dei Lincei, 25, suppl. 2, 241-252.

Giano S.I. & Schiattarella M. (2014) - *Age constraints and denudation rate of a multistage fault line scarp: an example from southern Italy*. Geochronometria, 41 (3), 245-255.

Giano S.I., Pescatore E., Agosta F., Prosser G. (2018) - *Geomorphic evidence of Quaternary tectonics within an underlap fault zone of southern Apennines, Italy*. Geomorphology, 303, 172-190.

Hack J.T. (1973) - *Stream-profile analysis and stream-gradient index*. Journal of Research of the U.S. Geological Survey, 1, 421-429.

Hare P.W. & Gardner T.W. (1985) - *Geomorphic indicators of vertical neotectonism along converging plate margins, Nicoya Peninsula, Costa Rica*. In: Morisawa M. & Hack J.T. (Eds.), *Tectonic Geomorphology*. Proceedings of the 15th Annual Bighamton Geomorphology Symposium. Allen & Unwin, Boston, 75-104.

Harkins N.W., Anastasio D.J., & Pazzaglia F.J. (2005) - *Tectonic geomorphology of the Red Rock fault, insights into segmentation and landscape evolution of a developing range front normal fault.* Journal of Structural Geology, 27, 1925-1939.

Holbrook J. & Schumm S.A. (1999) - *Geomorphic and sedimentary response of rivers to tectonic deformation: a brief review and critique of a tool for recognizing subtle epirogenic deformation in modern and ancient settings*. Tectonophysics, 305, 287-306.

Isacks B.L. (1992) - *"Long-term" land surface processes: Erosion, tectonics and climate history in mountain belts*. In: Mather P.M. (Ed.), *Terra-1 Understanding the Terrestrial Environment*, Taylor and Francis, London, 21-36.

ISIDe working group (2016) - *Italian Seismic Instrumental and parametric Data-base*. version 1.0. doi: 10.13127/ISIDe.

Keller E.A. & Pinter N. (2002) - *Active tectonics: Earthquakes, Uplift and Landscape*. Prentice Hall, Upper Saddle River, NJ., 362 pp.

Keller E.A., Zepeda R.L., Rockwell T.K., Ku T.L. & Dinklage W.S. (1998) - *Active tectonics at Wheeler Ridge, southern San Joaquin Valley, California*. Geological Society American Bulletin, 110, 298-310.

Kirby E. & Whipple K.X. (2012) - *Expression of active tectonics in erosional landscapes*. Journal of Structural Geology, 44, 54-75.

Labriola M., Onofrio V., Gallicchio S. & Tropeano M. (2008) - *Caratteri stratigrafico-strutturali della porzione frontale dell'Appennino lucano compresa fra Acerenza e Oppido Lucano (Potenza, Basilicata)*. Memorie Descrittive della Carta Geologica d'Italia, 77, 111-118.

Martino C., Nico G. & Schiattarella M. (2009) - *Quantitative analysis of InSAR Digital Elevation Models for identification of areas with*

different tectonic activity in southern Italy. Earth Surface Processes and Landforms, 34, 3-15.

Martino S., Bozzano F., Capoross I P., D'angiò D., Della Seta M., Esposito C., Fantini A., Fiorucc I M., Giannini L.m., Iannucc I R., Marmoni G.m., Mazzanti P., Miss Ori C., Moretto S., Rivellino S., Walter Romeo R.w., Sarandrea P., Schilirò L., Troiani F. & Varone C. (2017) - *Ground effects triggered by the 24th August 2016*, Mw 6.0 Amatrice (Italy) earthquake: surveys and inventorying to update the CEDIT catalogue. Geografia Fisica e Dinamica Quaternaria, 40 (1), 77-95.

Masek J.G., Isacks B.L., Gubbels T.L. & Fielding E.J. (1994) - Erosion and tectonics at the margins of continental plateaus. Journal of Geophysical Research, 99, 13,941-13,956

Matoš B., Pérez-Peña J.V. & Tomljenović B. (2016) - *Landscape response to recent tectonic deformation in the SW Pannonian Basin: Evidence from DEM-based morphometric analysis of the Bilogora Mt. area, NE Croatia*. Geomorphology, 263, 132-155.

Melosh B.L. & Keller E.A. (2013) - *Effects of active folding and reverse faulting on stream channel evolution, Santa Barbara Fold Belt, California*. Geomorphology, 186, 119-135.

Merrits D. & Vincent K.R. (1989) - *Geomorphic response of coastal streams to low, intermediate, and high rates of uplift, Mendocino triple junction region, northern California*. Geological Society American Bulletin, 101, 1373-1388.

Ntokos D., Lykoudi E. & Rondoyanni T. (2016) - *Geomorphic analysis in areas of low-rate neotectonic deformation: South Epirus (Greece) as a case study*. Geomorphology, 263, 156-169.

Ouchi S. (1985) - *Response of alluvial rivers to slow active tectonic movement*. Geological Society American Bulletin, 96, 504-515.

Papanikolaou I.D., Van Balen R., Silva P.G. & Reicherter K. (2015) - *Geomorphology of active faulting and seismic hazard assessment: New tools and future challenges.* Geomorphology, 237, 1-13.

Patacca E. & Scandone P. (2007) - *Geology of the Southern Apennines.* In: Mazzotti A., Patacca E., Scandone P. (Eds.), CROP-04. Bollettino della Società Geologica Italiana, Special Issue 7, 75-119.

Pedrera A., Pérez-Peña J.V., Galindo-Zaldívar J., Azañón J.M. & Azor A. (2009) - *Testing the sensitivity of geomorphic indices in areas of low-rate active folding (eastern Betic Cordillera, Spain)*. Geomorphology, 105, 218-231.

Pérez-Peña J.V., Azañón J.M., Azor A., Delgado J. & González-Lodeiro F. (2009) - *Spatial analysis of stream power using GIS: SLk anomaly maps*. Earth Surface Processes and Landforms, 34, 16-25.

Pérez-Peña J.V., Azor A., Azañón J.M. & Keller E.A. (2010) - *Active tectonics in the Sierra Nevada (Betic Cordillera, SE Spain): Insights from geomorphic indexes and drainage pattern analysis*. Geomorphology, 119, 74-87.

Pierce K.L. & Morgan L.A. (1992) - *The track of the Yellowstone hot spot: volcanism, faulting, and uplift.* In: Link P.K., Kuntz M.A., Platt L.B. (Eds.), *Regional Geology of Eastern Idaho and Western Wyoming*, Geological Society of America Memories, 179, 1-52.

Pieri P., Gallicchio S., Sabato L. & Tropeano M. (2011) - *Note illustrative della Carta Geologica d'Italia alla scala 1:50.000, Foglio 471 Irsina*. ISPRA, Servizio Geologico d'Italia, 112 pp.

Riviello A., Schiattarella M. & Vaccaro M.P. (1997) - *Struttura geologica dell'area di Tolve (Basilicata) dedotta da dati di superficie e di sottosuolo*. Il Quaternario, 10, 557- 562.

Schiattarella M., Beneduce P., Di Leo P., Giano S.I., Giannandrea P. & Principe C. (2005) - *Assetto strutturale ed evoluzione morfotettonica quaternaria del vulcano del Monte Vulture (Appennino Lucano)*. Bollettino della Società Geologica Italiana, 124, 543-562.

Schiattarella M., Di Leo P., Beneduce P., Giano S.I. & Martino C. (2006) - *Tectonically driven exhumation of a young orogen: An example from the southern Apennines, Italy*. In: Willett S.D., Hovius N., Brandon M.T., and Fisher D.M. (Eds.), *Tectonics, climate, and landscape evolution,* Geological Society of America, Special Paper 398, Penrose Conference Series, 371-385.

Schiattarella M., Giano S.I. & Gioia D. (2017) - *Long-term geomorphological evolution of the axial zone of the Campania-Lucania Apennine, Southern Italy: a review*. Geologica Carpathica, 68 (1), 57-67.

Schiattarella M., Giano S.I., Gioia D., Martino C. & Nico G. (2013) - *Age and statistical properties of the summit palaeosurface of southern Italy*. Geografia Fisica e Dinamica Quaternaria, 36, 289-302.

Schumm S.A. (1986) - *Alluvial River Response to Active Tectonics*. In: *Studies in Geophysics. Active Tectonics*. National Academy Press, Washington, 80-94.

Schumm S.A. (1977) - *The fluvial system*. John Wiley and Sons, New York, 338 pp.

Seeber L. & Gornitz V. (1983) - *River profiles along the Himalayan arc as indicators of active tectonics.* Tectonophysics, 92, 335-367.

Silva P.G., Goy J.L., Zaz C. & Bardajm T. (2003) - *Fault generated mountain fronts in Southeast Spain: geomorphologic assessment of tectonic and earthquake activity*. Gemorphology, 250, 203-226.

Soto R., Martinod J., Riquelme R., Hérail G. & Audin L. (2005) - *Using gemorphological markers to discriminate Neogene tectonic activity in the Precordillera of North Chilean forearc (24-25° S)*. Tectonophysics, 411, 41-55.

Stokes M., Cunha P.P. & Martins A.A. (2012) - *Techniques for analysing Late Cenozoic river terrace sequences*. Geomorphology, 165-166, 1-6.

Troiani F. & Della Seta M. (2008) - *The use of the stream length-gradient index in morphotectonic analysis of small catchments: a case study from Central Italy*. Geomorphology, 102, 159-168.

Troiani F., Galve J.P., Piacentini D., Della Seta M. & Guerrero J. (2014) - *Spatial analysis of stream length-gradient (SL) index for detecting hillslope processes: A case of the Gállego River headwaters (Central Pyrenees, Spain)*. Geomorphology 214, 183-197.

Watson D.F. & Philip G.M. (1985) - *A refinement of inverse distance weighted interpolation*. Geo-Processing, 2, 315- 327.

Wells S.G., Bullar T.F., Menges C.M., Drake P.G., Kara P.A., Kelson K.I., Ritter J.B. & Wesling J.R. (1988) - *Regional variations in tectonic geomorphology along a segmented convergent plate boundary, Pacific coast of Costa Rica.* Geomorphology, 1, 239-365.

(Ms. received 20 November 2017; accepted 15 May 2018)